JOURNAL OF ENVIRONMENTAL SCIENCES 95 (2020) 91–98

Available online at www.sciencedirect.com

ScienceDirect

www.elsevier.com/locate/jes

JES JOURNAL OF ENVIRONMENTAL SCIENCES

www.jesc.ac.cn

Pollution sources of atmospheric fine particles and secondary aerosol characteristics in Beijing

Xi Zhang[1,2,3], *Kai Zhang*[1,*], *Huiping Liu*[4], *Wenli Lv*[1], *Masahide Aikawa*[3], *Bing Liu*[5], *Jinhe Wang*[2,6,*]

[1] *State Key Laboratory of Environmental Criteria and Risk Assessment, Chinese Research Academy of Environmental Sciences, Beijing 100012, China*

[2] *School of Municipal and Environmental Engineering, Co-Innovation Center for Green Building of Shandong Province, Shandong Jianzhu University, Jinan 250101, China*

[3] *Faculty of Environmental Engineering, The University of Kitakyushu, 1-1, Hibikino, Wakamatsu, Kitakyushu, Fukuoka 808-0135, Japan*

[4] *Qingdao Hongrui Electric Power Engineering Consulting Co., Ltd, Qingdao 266100, China*

[5] *Resources and Environment Innovation Research Institute, School of Municipal and Environmental Engineering, Shandong Jianzhu University, Jinan 250101, China*

[6] *Shanghai Key Laboratory of Atmospheric Particle Pollution and Prevention (LAP3), Department of Environmental Science and Engineering, Fudan University, Shanghai 200438, China*

ARTICLE INFO

Article history:
Received 15 September 2019
Revised 27 March 2020
Accepted 1 April 2020
Available online 16 April 2020

Keywords:
Water-soluble ions
Secondary aerosols
Potential source
Gaseous precursors
Sensitive analysis

ABSTRACT

To investigate the secondary formation and pollution sources of atmospheric particles in urban Beijing, $PM_{2.5}$ and its chemical components were collected and determined by URG-9000D ambient ion monitor (AIM) from March 2016 to January 2017. Among water-soluble ions (WSIs), NO_3^-, SO_4^{2-} and NH_4^+ (SNA) had the largest proportion (77.8%) with the total concentration of 23.8 μg/m^3. Moreover, as fine particle pollution worsened, the NO_3^-, SO_4^{2-} and NH_4^+ concentrations increased basically, which revealed that secondary aerosols were the main cause of particle pollution in Beijing. Furthermore, the particle neutralization ratio (1.1), the ammonia to sulfate molar ratio (3.4) and the nitrate to sulfate molar ratio (2.2) showed that secondary aerosols are under ammonium-rich conditions with the main chemical forms of NH_4NO_3 and $(NH_4)_2SO_4$, and vehicle emission could be the main anthropogenic source of secondary aerosols in Beijing. Source analysis further indicated that secondary aerosols, solid fuel combustion, dust and marine aerosol were the principal pollution sources of $PM_{2.5}$, accounting for about 46.1%, 22.4% and 13.0%, respectively, and Inner Mongolia and Hebei Provinces could be considered as the main potential sources of $PM_{2.5}$ in urban Beijing. In addition, secondary formation process was closely related with gaseous precursor emission amounts (SO_2, NO_2, NH_3 and HONO), atmospheric ozone concentration (O_3), meteorological conditions (temperature and relative humidity) and particle components. Sensitive analysis of the thermodynamic equilibrium model (ISORROPIA II)

* Corresponding authors.
E-mails: zhangkai@craes.org.cn (K. Zhang), jinhewang@263.net, jhw@sdjzu.edu.cn (J. Wang).

https://doi.org/10.1016/j.jes.2020.04.002

revealed that controlling total nitrate (TN) is the effective measure to mitigate fine particle pollution in Beijing.

Introduction

Atmospheric particle is a complex mixture of primary particles emitted directly from natural and anthropogenic activities and secondary particles produced by gas-to-particle conversion processes, which strongly affects the atmospheric radiation balance, visibility, precipitation acidity and cloud formation process, finally affects regional and global climate and causes human health problems as well (Hama et al., 2017; Kim and Zhang, 2019; Pietrogrande et al., 2018; Quan et al., 2015; Svedova et al., 2019; Wang et al., 2017; Zhang et al., 2019). The size distribution and chemical compositions of atmospheric particles play an essential role in their transport, transformation, evolution and removal mechanisms in the atmosphere (Kleeman et al., 2009; Liu et al., 2016). Over the last decade, the pollution of atmospheric fine particle has raised great attention due to the occurrence of frequent and persistent large-scale haze episodes in China, especially in the North China Plain (Ding et al., 2019; He et al., 2014). Since 2013, the government has taken increasingly strict particle control measures, especially limiting sulfur emissions (The National Ambient Air Quality Standard of China (GB 3095-2012) and The Action Plan for Air Pollution Prevention and Control (2013-2017)), which have achieved marked improvements in air quality as of 2017 (Zong et al., 2018). However, the fine particle pollution still remains far from being controlled, especially in Beijing. The concentration of $PM_{2.5}$ in Beijing (88.9 $\mu g/m^3$) was not significantly reduced after taking a series of pollutant emission reduction measures, moreover, the proportion contribution of SNA even increased (Du et al., 2018; Quan et al., 2015; Shang et al. 2018; Tian et al. 2016; Zong et al., 2018), which was closely related to the secondary aerosol formation process.

Although many researches have analyzed the specific relationship between the concentration of NO_3^-, SO_4^{2-} and NH_4^+ (SNA) and several influencing factors (gaseous precursors, oxidants or meteorological conditions) (Cheng and Li, 2010; Kitamori et al., 2009; Kong et al., 2018; Kudo et al., 2018; Mesquita et al., 2016; Tan et al., 2017; Wang et al., 2019a; Xu et al., 2017; Xue et al., 2014), the secondary aerosol formation studies focusing on the comprehensive influence of related factors were few, and the effective control measures are worth to be investigated. Moreover, the information about pollution sources and potential pollution regions of fine particles needs to be updated.

Year-round observation of $PM_{2.5}$ was carried out in urban area of Beijing and this study investigated the characteristics of water-soluble inorganic ions, and analyzed secondary aerosol formation mechanism combined with gaseous pollutants (SO_2, NO_2, NH_3, HONO, O_3, etc.) and meteorological factors (temperature (*T*) and relative humidity (RH)) by using Pearson correlation analysis and thermodynamic equilibrium model (ISORROPIA II). The main objectives of this study are (1) to assess the sources of atmospheric fine particle in urban Beijing and distinguish the pollution regions based on PCA (principal component analysis) and WCWT (weighted concentration weighted trajectory) analysis; (2) to analyze the influencing factors of secondary aerosol formation process and find an effective measure to mitigate secondary aerosols pollution. The finding of this study provides a significant field measurement-based evidence, and thus facilitates air quality improvement policy formulation in urban area of Beijing.

1. Materials and methods

1.1. Experimental

The sampling campaign was carried out on the rooftop of Smog Chamber Building at the Chinese Research Academy of Environmental Sciences (CRAES, 40°04.164′N and 116°41.551′E) from March 2016 to January 2017. The sampling site is neighboring a residential area, which is in the middle of the north section of the 5th Ring Road of urban Beijing.

The URG-9000D ambient ion monitor (AIM) (Thermo Fisher Scientific, USA) was used to measure the concentrations of WSIs (Cl^-, NO_3^-, SO_4^{2-}, Na^+, NH_4^+, K^+, Mg^{2+} and Ca^{2+}) in $PM_{2.5}$ and gases precursors (SO_2, HONO, NH_3) with a time resolution of 1 hr. This instrument is installed 10 m above the ground and consists of the sampling system, analytical system and data collection system. First, the ambient air sample passed through a $PM_{2.5}$ cyclone and external inlet tube to enter the collection part of sampling system. During this process, the flow rate was 3 L/min, and the cross-linked Teflon coated aluminum tube was used to reduce the sample loss on the tubing walls. In collection part, the gases and particles were effectively absorbed by the wet parallel plate denuder (WPPD) and the steam jet aerosol collector (SJAC) with a sampling efficiency of 99%. Then the water-soluble components of particle and gases were extracted by a hydrogen peroxide solution, and the solutions were analyzed by two ion chromatographs (ICS-1000, Dionex, USA). Finally, the hourly values of particle components and gases were collected in real time by the computer. In addition, the air pollutants (SO_2, NO_2, O_3, CO, $PM_{2.5}$, NH_3) and meteorological data (*T* and RH) were simultaneously obtained using Model 43i SO_2 analyzer (Thermo Fisher Scientific, USA), Model 17i NO_x analyzer (Thermo Fisher Scientific, USA), Model 49i O_3 analyzer (Thermo Fisher Scientific, USA), Model 48i CO analyzer (Thermo Fisher Scientific, USA), Model 5030 SHARP monitor (Thermo Fisher Scientific, USA), G2103 (Picarro, USA), and MAWS110 (Vaisala, Finland).

1.2. Quality assurance and quality control

Strict quality control of the instrument (AIM) was carried out to ensure data quality during the whole monitoring period. The sampling flow was calibrated regularly, and the standard curves were made every two months to keep the correlation coefficients remain above 0.999 for every ion. The range of detection limits was between 0.0025 and 0.02 $\mu g/m^3$. In addition, the WSIs, SO_2 and NH_3 measured by AIM were compared with the $PM_{2.5}$, SO_2 and NH_3 obtained by other online monitoring instruments at the same site during the same sampling period. The results indicated that the WSIs and $PM_{2.5}$ mass concentrations showed similar variation trends, and the $PM_{2.5}$ mass concentrations were generally higher than those of WSIs with the slope of 3.1 and the correlation coefficient (R^2) of 0.7. Moreover, the variation trends of SO_2 (or NH_3) measured by different instruments agreed well, with the R^2 value larger than 0.8.

Table 1 – Average concentration of particle components (μg/m³) and three gaseous pollutants (ppbV) in four seasons.

Season (Sampling period)	$PM_{2.5}$	WSIs	SNA	Na^+	Cl^-	K^+	Mg^{2+}	Ca^{2+}	NO_2	SO_2	NH_3
Spring (March-May, 2016)	95.7	31.8	24.8	1.3	2.8	0.9	0.2	1.8	30.7	2.4	21.4
Summer (June-August, 2016)	61.1	24.5	20.9	1.8	0.7	0.5	0.1	0.5	16.3	1.1	38.5
Autumn (September-November, 2016)	82.0	29.1	25.8	1.2	0.9	0.6	0.1	0.5	29.6	3.0	20.3
Winter (December 2016-January 2017)	133.1	37.9	26.9	4.4	3.8	0.3	0.5	2.0	43.6	10.1	12.2

WSIs: water-soluble ions; SNA: NO_3^-, SO_4^{2-} and NH_4^+.

1.3. *Statistical analysis and model calculation*

1.3.1. *Principal component analysis (PCA) and hierarchical cluster analysis (HCA)*

Statistical calculations were performed using the IBM SPSS Statistics 20.0. In this study, emission sources of $PM_{2.5}$ were identified using PCA and HCA techniques. The input data included the concentrations of 8 particle components (Na^+, Ca^{2+}, Mg^{2+}, K^+, NH_4^+, SO_4^{2-}, NO_3^-, Cl^-) in each samples. As for PCA, the principle of extracting principal component number is the cumulative percentage larger than 80%. Factor loadings showed the correlations of eight variables with principal components, providing the information of source emission composition (Liu et al., 2018; Oliva and Espinosa, 2007; Siepka et al., 2018; Skrbic and Durisic-Mladenovic, 2007; Xue et al., 2011; Zhong et al., 2016). As for HCA, average group and squared Euclidean distance were used as the linkage method and dissimilarity metric. Values were standardized (by variables) using Z scores (Chen et al., 2016; Kudo et al., 2018; Mesquita et al., 2016; Pietrogrande et al., 2018; Siepka et al., 2018; Tang and Han, 2017; Zhong et al., 2016).

1.3.2. *Hybrid single-particle Lagrangian integrated trajectory model (HYSPLIT) and weighted concentration-weighted trajectory (WCWT)*

The 48-hr backward trajectories were generated by HYSPLIT model of TrajStat Software based on GDAS data. The arriving height and top of the model are 1000 and 10,000 m, respectively. Then the cluster analysis and WCWT analysis were performed in this study to investigate the transport pathways and potential sources of $PM_{2.5}$ in four seasons (Kong et al., 2018; Nakahara et al., 2019; Roig Rodelas et al., 2019; Tan et al., 2017; Tang et al., 2016; Wang et al., 2019a).

1.3.3. *Thermodynamic model*

The thermodynamic inorganic model, ISORROPIA II, was used to simulate multiphase chemical reactions after controlling secondary aerosols emission. The forward mode and metastable phase state were finally chosen in this model with the input data of total ammonia ($NH_3 + NH_4^+$), total nitrate ($HNO_3 + NO_3^-$), total chloride ($HCl + Cl^-$), other particle components concentrations (Na^+, Ca^{2+}, Mg^{2+}, K^+ and SO_4^{2-}) and meteorological factors (*T* and RH) (Karydis et al., 2010; Sudheer and Rengarajan, 2015).

2. Results and discussion

2.1. *Concentration characteristics*

During the sampling period (Table 1), the average mass concentration of $PM_{2.5}$ was 88.9 ± 99.0 μg/m³, and had obvious seasonal variation with the highest concentration in winter (133.1 μg/m³), followed by spring (95.7 μg/m³), autumn (82.0 μg/m³) and summer (61.1 μg/m³). Among particle components, WSIs accounted for 28.5%-40.1% of particle mass concentration in four seasons, and the average mass concentrations of Cl^-, NO_3^-, SO_4^{2-}, Na^+, NH_4^+, K^+, Mg^{2+}, and Ca^{2+} were 2.5, 9.8, 6.4, 2.2, 7.6, 0.6, 0.2, and 1.3 μg/m³, respectively. The high proportion (77.8%) of SNA in the total concentration of WSIs indicated that secondary aerosols was the significant pollution source of the atmospheric fine particle in urban Beijing, which was consistent with previous studies (Li et al., 2013, 2016; Tian et al., 2018; Wang et al., 2019b). The particle neutralization ratio ($n(NH_4^+)/(2n(SO_4^{2-})+n(NO_3^-))$) was 1.1, and the ammonia to sulfate molar ratio ($n(NH_4^+)/n(SO_4^{2-})$) was 3.4, which revealed that secondary aerosols were under ammonium-rich conditions and NH_4^+ was mainly with the main chemical forms of NH_4NO_3 and $(NH_4)_2SO_4$ in Beijing (Makar et al., 2009; Yin et al., 2018). NO_2 and SO_2 had similar seasonal variations with NO_3^- and SO_4^{2-}, and showed strong correlations with $PM_{2.5}$ at the significant level of 0.01, with the correlation coefficients of 0.8 and 0.6, respectively. Moreover, the molar ratio of NO_3^- to SO_4^{2-} (2.2) was larger than 1, revealing that the industrial restructuring and industrial emission desulfurization in Beijing have been very effective in reducing SO_2 emissions, but vehicle emissions has gradually become a main particle pollution source (Huang et al., 2016). In addition, NH_3 had different seasonal variation with NO_2 and SO_2, with the highest concentration in summer, followed by spring and summer, and the lowest concentration in winter, which were mainly influenced by the intensity of emission source and thermodynamic equilibrium between gas and particle (Jiang and Xia, 2017; Li et al., 2018; Osada et al., 2019).

To investigate the variation of WSIs with different air quality levels, the samples were further classified as excellent clean, clean, slight pollution, moderate pollution and severe pollution levels based on the Technical Regulation on Ambient Air Quality Index of China (HJ633-2012), and the corresponding AQI (air quality index) is <50, 51-100, 101-150, 151-200 and >201, respectively. The proportions of WSIs at five air quality levels was shown in Fig. 1. It can be seen that SNA accounted for 54.8%, 75.7%, 84.3%, 83.2% and 90.7% of the total WSIs at excellent clean, clean, slight pollution, moderate pollution and severe pollution levels, respectively. To be specific, the proportion of NO_3^- and NH_4^+ increased gradually with the increase of pollution grade, ranging from 16.2% to 37.2% and 23.0% to 28.4%, respectively. Different from NO_3^- and NH_4^+, SO_4^{2-} proportion gradually increased from excellent clean to slight pollution level (15.6% to 26.2%), while the proportion did not continue to rise at moderate pollution (22.3%) and severe pollution levels (25.1%). In addition, other ions (Na^+, Cl^-, K^+, Mg^{2+} and Ca^{2+}) basically decreased with the increase of pollution grade because of the predominant influence of SNA.

2.2. *Source apportionment*

The main sources of collected $PM_{2.5}$ in Beijing was determined by PCA. Three components were extracted as principal components, which could explain the 81.5% of the total

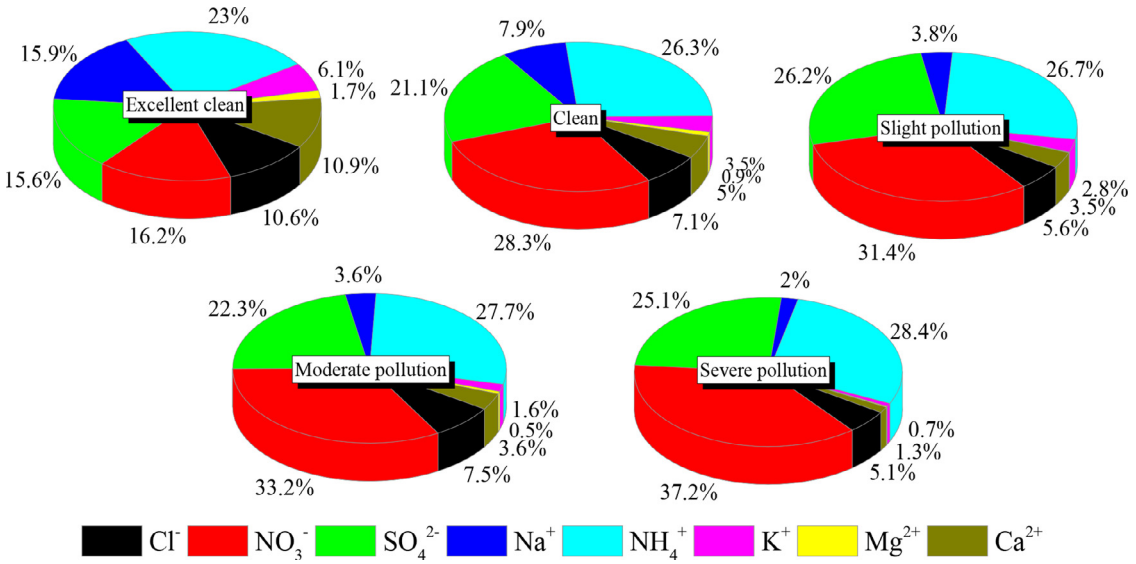

Fig. 1 – Proportions of WSIs at different air quality levels.

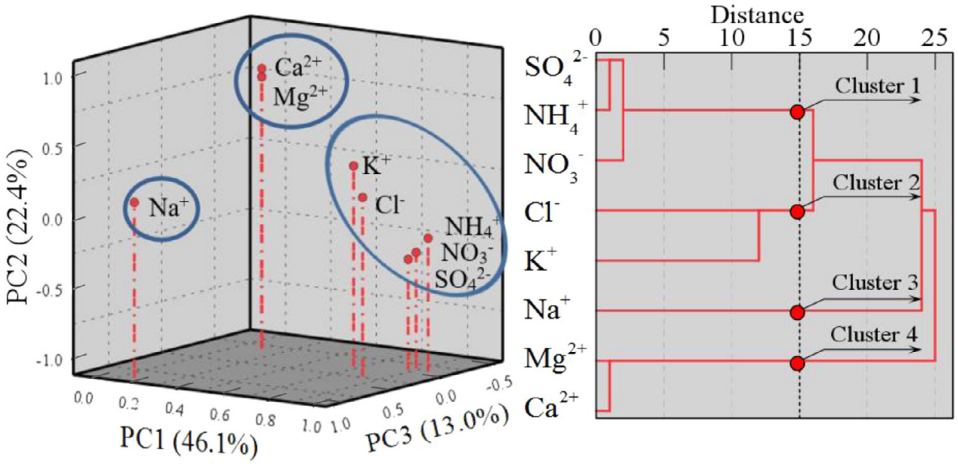

Fig. 2 – Principal component analysis (PCA, left) and hierarchical cluster analysis (right) of eight WSIs in atmospheric fine particle in Beijing.

variance. The factor loadings between principal components and eight variables are shown in Fig. 2. PC1 (The first principal component) explained the 46.1% of the total variance and was typically characterized by high factor loading (>0.8) of NH_4^+, NO_3^-, SO_4^{2-} and Cl^-, revealing the influence of secondary aerosols from the anthropogenic sources (vehicle emission and coal combustion). The relatively high loading of K^+ (0.7) in PC1 may be associated with biomass burning which is the anthropogenic source for the emission of gaseous precursors (SO_2 and NO_x) (Saxena et al., 2017). In addition, this mixed source had obvious seasonal variation, with larger contribution in spring (56.0%) and winter (55.3%) and relatively lower contribution in summer (44.6%) and autumn (41.9%). PC2 (the second principal component) was closely associated with Ca^{2+} and Mg^{2+} with the factor loading of 0.9 and 0.8, respectively, and contributed for 22.4% of total sources. This source may be originated from desert dust from Inner Mongolia, and anthropogenic construction dust, fugitive dust, resuspended road dust near sampling site. PC3 (the third principal component) can be defined as marine aerosol because of the high factor loading of Na^+ (0.9), and accounted for 13.0% of the total variances. The source results of PCA are in good agreement with those of the HCA, as shown in Fig. 2. The distances reflect the degree of association between different WSIs and the cut line in this study was at the distance of 15. Hence eight WSIs were further classified and merged into four distinct clusters: (1) NO_3^-, NH_4^+ and SO_4^{2-} (secondary aerosols); (2) Cl^- and K^+ (solid fuel combustion); (3) Mg^{2+} and Ca^{2+} (dust); (4) Na^+ (marine aerosol).

2.3. *Transport pathway and potential source*

Atmospheric particles could be carried by long-distance transporting air masses and cause predominant effect on the sampling site which was even far away from the emission source, thus the air quality of the sampling site could be affected not only by the nearby area but also the areas along the transport pathways of particles. As trajectory presented (Fig. 3), in spring, the air masses mainly transported northwesterly, including Clusters 1, 3 and 4, which had the highest proportion (73.9%) in total clusters. In contrast, the transported air masses from southwest (Cluster 5) and southeast

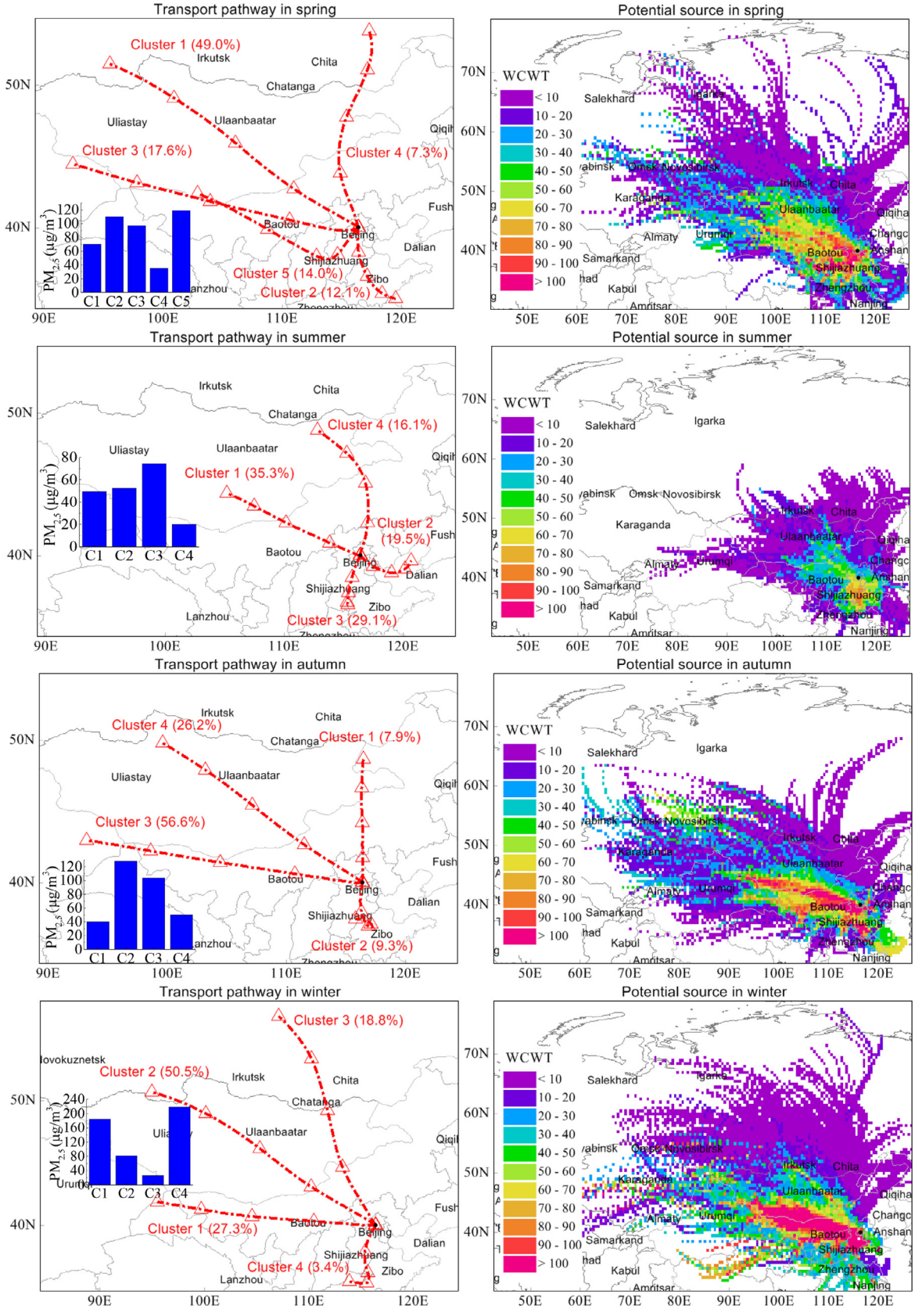

Fig. 3 – Cluster analysis and weighted concentration-weighted trajectory (WCWT) analysis of fine particles in four seasons.

Table 2 – Statistics of gaseous pollutants' average concentration under different clusters.

Season	Cluster	SO_2 (ppbV)	NO_2 (ppbV)	NH_3 (ppbV)	HONO (ppbV)	O_3 (ppbV)	CO (ppmV)
Spring	1	2.9	23.2	20.0	1.2	26.2	3.2
	2	4.1	30.8	26.0	1.8	29.2	3.5
	3	2.5	25.3	31.9	1.9	46.0	3.5
	4	2.2	17.0	15.7	0.6	24.6	3.3
	5	2.9	28.7	30.0	1.5	30.7	3.5
Summer	1	1.1	17.0	40.1	1.3	45.6	1.9
	2	1.1	16.5	34.4	1.2	47.8	2.0
	3	1.4	17.8	38.0	1.6	51.7	1.9
	4	0.9	16.1	34.5	0.7	37.1	2.0
Autumn	1	2.4	20.8	22.0	0.9	18.8	3.7
	2	4.8	35.3	57.3	1.7	14.1	5.1
	3	5.1	37.3	19.2	1.9	13.1	5.2
	4	4.2	26.4	18.5	1.0	17.8	4.7
Winter	1	12.1	46.9	12.7	3.8	4.2	8.9
	2	6.1	27.0	9.3	2.1	14.1	5.8
	3	2.7	15.0	6.2	1.3	20.3	3.5
	4	17.9	51.8	18.0	5.4	5.6	10.4

(Cluster 2) only accounted for 14.0% and 12.1%, respectively, but these air masses carried the highest concentrations of fine particles (117.3 and 110.7 $\mu g/m^3$) as well as the highest SO_2 and NO_2 concentrations (Table 2). WCWT analysis further indicated that the high concentrations of fine particles in southern area of Hebei Province had predominant influence on the particle pollution of Beijing in spring. In summer, the air masses were derived from four clustering directions (northwest, southeast, southwest and northeast), occupying 35.3%, 19.5%, 29.1% and 16.1%, respectively. In particular, Clusters 1 and 4 were originated from Mongolia, passing through Inner Mongolia, Hebei Provinces of China and finally reached sampling site. Cluster 2 came from the Bohai Sea, passing through Tianjin, then entered Beijing. While, Cluster 3 indicated the influence of particles from Heibei Province, carrying the highest concentration of $PM_{2.5}$ (74.2 $\mu g/m^3$), SO_2 (1.4 ppbV), NO_2 (17.8 ppbV), HONO (1.6 ppbV), and O_3 (51.7 ppbV) than other three clusters. Same as spring, WCWT analysis showed that the southern regions of Hebei Province had relative high influence on the particle pollution of Beijing in summer, but the air quality was obviously better than that in spring. In autumn, the northerly and northwesterly transported air parcels (Clusters 1 and 4) from Mongolia were relative clean with the $PM_{2.5}$ concentrations of 40.7 and 52.1 $\mu g/m^3$, respectively. The concentrations of $PM_{2.5}$ and gaseous pollutants carried by southerly transported air parcels from Shandong and Hebei Provinces, China (Cluster 2) and westerly transported air parcels from Inner Mongolia (Cluster 3) were obviously higher than that carried by Clusters 1 and 4, except for O_3. Furthermore, because of the highest proportion of Cluster 3 (56.6%), Inner Mongolia was considered as the main potential source of $PM_{2.5}$ in autumn. In winter, even the westerly transported air parcels from Inner Mongolia (Cluster 1) and southwesterly short-distance transporting air parcels from Shandong and Hebei Provinces, China (Cluster 4) only together accounted for 30.7%, the concentration of $PM_{2.5}$ carried by these two clusters were 185.0 and 218.9 $\mu g/m^3$, respectively, which were obviously higher than that carried from northwest (Clusters 2 and 3), as well as the much higher gaseous precursors concentrations (SO_2, NO_2, NH_3, HONO and CO) Clusters 1 and 4 carried than that of Clusters 2 and 3. Moreover, WCWT analysis distinguished the particle pollution sources distributed in western and nearby southern areas of sampling sites, where various industries are spread in the west and the most populated district is just located in the south.

2.4. *Secondary aerosol characteristics*

The sulfur oxidation rate and nitrogen oxidation rate (SOR and NOR) were often used to evaluate the oxidation and secondary formation degree in the atmosphere (Svedova et al., 2019; Xu et al., 2017; Zhou et al., 2016). During the whole monitoring period, the SOR and the NOR values were 0.3, and 0.1, respectively, while during polluted periods (AQI > 100), the SOR and the NOR values increased 80% and 50%, respectively, suggesting that secondary formation is the significant cause of particle pollution in Beijing.

Pearson coefficient analysis (Table 3) indicated that secondary formation process can be affected by various influencing factors. Specifically, among gaseous pollutants, SOR and NOR all had positive correlation with NH_3 and O_3. This phenomenon revealed that the increase of NH_3 and O_3 concentration may enhance secondary aerosols formation, especially

Table 3 – Pearson analysis on sulfur oxidation rate (SOR) and nitrogen oxidation rate (NOR).

Pearson coefficient	SOR	NOR
SO_2	-	-0.1
NO_2	-0.1	-
NH_3	0.7**	0.5**
HONO	0.1	0.3**
O_3	0.6**	0.3**
RH	0.6**	0.4**
T	0.6**	0.2*
SO_4^{2-}	-	0.6**
NO_3^-	0.5**	-
NH_4^+	0.6**	0.6**
Na^+	-0.1	-0.1
Cl^-	-0.1	0.1
K^+	0.5**	0.4**
Mg^{2+}	-0.3**	-0.1
Ca^{2+}	0.0	-0.1

SOR = $n(SO_4^{2-})/(n(SO_4^{2-}) + n(SO_2))$; NOR = $n(NO_3^-)/(n(NO_3^-) + n(NO_2^-))$; $n(x)$ ($\mu mol/m^3$) refers to the molar concentration of the species (x); - means the parameter to calculate SOR or NOR;
** $p < 0.01$;
* $p < 0.05$.

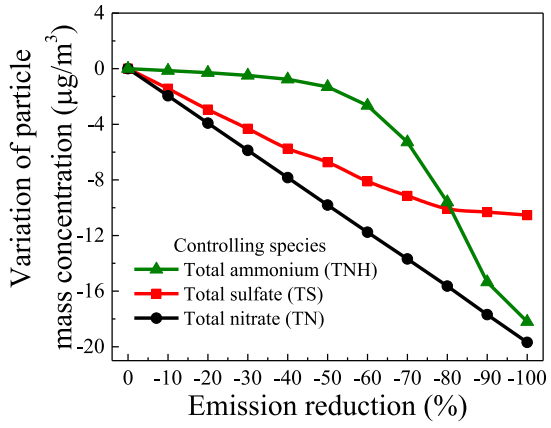

Fig. 4 – Variation of particle mass concentration after implementing different control measures.

the secondary formation of sulfate. High levels of NH_3 can sufficiently elevate aerosol pH to promote rapid sulfate formation, and high concentration of O_3 can also enhance the contribution of photochemistry to the secondary sulfate formation (Guo et al., 2017; Jiang et al., 2019; Kong et al., 2018). In addition, NOR was also sensitive with the variation of HONO with the Pearson coefficient of 0.3. As for meteorological condition, SOR and NOR values increased with the simultaneous growth of relative humidity and temperature, but the correlation coefficient between NOR and *T* at 0.05 significant level was even obviously lower than that between SOR and *T* at 0.01 significant level. This phenomenon may be ascribed to the equilibrium shift of NH_4NO_3 to gaseous HNO_3 and NH_3 under high temperature (Schiferl, et al., 2016; Watson, et al., 1994). Particle properties also had effect on secondary formation process. In particular, the existence of SO_4^{2-} and NO_3^- in fine particles could also enhance the secondary formation of nitrate and sulfate, respectively, and NH_4^+, as the primary alkaline species in particles, had positive coefficient with SOR and NOR, respectively. Among other particle components, K^+ had the highest positive coefficients with SOR (0.5) and NOR (0.4) at the significant level of 0.01, while Mg^{2+} can depress the secondary formation of sulfate.

To find the optimal control measure to mitigate secondary aerosols pollution, ISORROPIA II was performed with the forward mode (HNO_3 and HCl were excluded) and metastable phase state (Karydis et al., 2010; Sudheer and Rengarajan, 2015). The sensitivity of emission reduction of total sulfate, nitrate and ammonium (TS, TN and TNH), respectively, on fine particle mass concentration (Fig. 4) showed that the concentration variation of fine particle mass after controlling TN was the largest than that of controlling TS and TNH, respectively. Hence emission reduction of total nitrate was the most efficient measure to mitigate fine particle pollution. In addition, when the reduction ratio was lower than 50%, controlling the emission of total ammonium basically had no obvious influence on fine particle mass concentration, while the decreasing rate of fine particle mass significantly increased with the reduction ratio when it was larger than 50%. Furthermore, when the reduction ratio was larger than 80%, controlling the emission of TNH was more effective than controlling the emission of TS.

3. Conclusions

We conducted the observation of $PM_{2.5}$ and gaseous pollutants in urban area of Beijing for almost one year to investigate particle characteristics, pollution sources and secondary aerosol formation process. The main conclusions are as follows:

(1) SNA accounted for 77.8% of total WSIs during sampling period, mainly with the chemical forms of NH_4NO_3 and $(NH_4)_2SO_4$, and secondary aerosol formation was significantly associated with not only the variations of SO_2 and NO_2, but also the variations of NH_3, HONO, O_3, *T*, RH and particle components.
(2) Particle pollution sources mainly included secondary aerosols plus solid fuel combustion (46.1%), dust (22.4%) and marine aerosol (13.0%) in this urban area in Beijing.
(3) Cluster analysis and WCWT analysis indicated that in-country transport of $PM_{2.5}$ had obviously higher influence on the air quality of sampling site than trans-boundary transport from Mongolia. Severe fine particle pollution was mainly caused by the local emissions from Inner Mongolia and Hebei Provinces, China, especially in winter.
(4) The sensitive analysis by ISORROPIA II indicated that emission reduction of total nitrate is the optimal control measure to mitigate fine particle pollution, followed by emission reduction of total sulfate and total ammonium, respectively, when the reduction ratio was lower than 80%.

In view of the above results, the mitigation policies for fine particle pollution in the urban area of Beijing should enhance the collaborative efforts of Inner Mongolia and Hebei provinces on particulate pollution control, and particularly focus on secondary aerosols reducing, especially through the emission reduction of total nitrate.

Declaration of competing interest

The authors declare that they have no known competing financial interests or personal relationships that could have appeared to influence the work reported in this paper.

Acknowledgments

This work was supported by the National Research Program for key issues in air pollution control (No. DQGG0304-05), the Fundamental Research Funds for Central Public Welfare Scientific Research Institutes of China (No. 2016YSKY-025), the National Department Public Benefit Research Foundation (No. 201109005), the National Natural Science Foundation of China (Nos. 41205093, 41305124, and 21976106), the Opening Project of Shanghai Key Laboratory of Atmospheric Particle Pollution and Prevention (No. FDLAP18005) and the National Key Research and Development Program of Ministry of Science and Technology of China (No. 2016YFE0112200). This work was also supported by Science Foundation of Shandong Jianzhu University (No. XNBS1824) and Shandong Key Research and Development Program (No. 2019GSF109064). Jinhe Wang appreciates the supports from the Co-Innovation Center for Green Building of Shandong Province (No. X18027Z) and the Introduction and Cultivation Plan for Young Innovative Talents of Colleges and Universities by the Education Department of Shandong Province (Serial No. 142, 2019).

REFERENCES

Chen, H.W., Chen, W.Y., Chang, C.N., Chuang, Y.H., Lin, Y.H., 2016. Identifying airborne metal particles sources near an optoelectronic and semiconductor industrial park. Atmos. Res. 174-175, 97–105.

Cheng, Y.H., Li, Y.S., 2010. Influences of traffic emissions and meteorological conditions on ambient PM_{10} and $PM_{2.5}$ levels at a highway toll station. Aerosol Air Qual. Res. 10, 456–462.
Ding, J., Zhang, Y.F., Zhao, P.S., Tang, M., Xiao, Z.M., Zhang, W.H., et al., 2019. Comparison of size-resolved hygroscopic growth factors of urban aerosol by different methods in Tianjin during a haze episode. Sci. Total Environ. 678, 618–626.
Du, J., Zhang, X., Huang, T., Gao, H., Mo, J., Mao, X., et al., 2018. Removal of $PM_{2.5}$ and secondary aerosols in the north China plain by dry deposition. Sci. Total Environ. 651, 2312–2322.
Guo, H., Weber, R.J., Nenes, A., 2017. High levels of ammonia do not raise fine particle pH sufficiently to yield nitrogen oxide-dominated sulfate production. Sci. Rep. 7, 12109.
Hama, S.M.L., Cordell, R.L., Monks, P.S., 2017. Quantifying primary and secondary source contributions to ultrafine particles in the UK urban background. Atmos. Environ. 166, 62–78.
He, H., Wang, Y., Ma, Q., Ma, J., Chu, B., Ji, D., et al., 2014. Mineral dust and NOx promote the conversion of SO_2 to sulfate in heavy pollution days. Sci. Rep. 4, 4172.
Huang, X., Liu, Z., Zhang, J., Wen, T., Ji, D., Wang, Y., 2016. Seasonal variation and secondary formation of size-segregated aerosol water-soluble inorganic ions during pollution episodes in Beijing. Atmos. Res. 168, 70–79.
Jiang, B., Xia, D., 2017. Role identification of NH_3 in atmospheric secondary new particle formation in haze occurrence of China. Atmos. Environ. 163, 107–117.
Jiang, F., Liu, F., Lin, Q., Fu, Y., Yang, Y., Peng, L., et al., 2019. Characteristics and formation mechanisms of sulfate and nitrate in size-segregated atmospheric particles from urban Guangzhou, China. Aerosol Air Qual. Res. 19, 1284–1293.
Karydis, V.A., Tsimpidi, A.P., Fountoukis, C., Nenes, A., Zavala, M., Lei, W., et al., 2010. Simulating the fine and coarse inorganic particulate matter concentrations in a polluted megacity. Atmos. Environ. 44, 608–620.
Kim, H., Zhang, Q., 2019. Chemistry of new particle growth during springtime in the Seoul metropolitan area, Korea. Chemosphere 225, 713–722.
Kitamori, Y., Mochida, M., Kawamura, K., 2009. Assessment of the aerosol water content in urban atmospheric particles by the hygroscopic growth measurements in Sapporo, Japan. Atmos. Environ. 43, 3416–3423.
Kleeman, M.J., Riddle, S.G., Robert, M.A., Jakober, C.A., Fine, P.M., Hays, M.D., et al., 2009. Source apportionment of fine ($PM_{1.8}$) and ultrafine ($PM_{0.1}$) airborne particulate matter during a severe winter pollution episode. Environ. Sci. Technol. 43, 272–279.
Kong, L., Du, C., Zhanzakova, A., Cheng, T., Yang, X., Wang, L., et al., 2018. Trends in heterogeneous aqueous reaction in continuous haze episodes in suburban Shanghai: An in-depth case study. Sci. Total Environ. 634, 1192–1204.
Kudo, S., Iijima, A., Kumagai, K., Tago, H., Ichijo, M., 2018. An exhaustive classification for the seasonal variation of organic peaks in the atmospheric fine particles obtained by a gas chromatography/mass spectrometry. Environ. Technol. Innov. 12, 14–26.
Li, K., Chen, L., White, S.J., Yu, H., Wu, X., Gao, X., et al., 2018. Smog chamber study of the role of NH_3 in new particle formation from photo-oxidation of aromatic hydrocarbons. Sci. Total Environ. 619-620, 927–937.
Li, X., Wang, L., Ji, D., Wen, T., Pan, Y., Sun, Y., et al., 2013. Characterization of the size-segregated water-soluble inorganic ions in the Jing-Jin-Ji urban agglomeration: Spatial/temporal variability, size distribution and sources. Atmos. Environ. 77, 250–259.
Li, Y., Tao, J., Zhang, L., Jia, X., Wu, Y., 2016. High contributions of secondary inorganic aerosols to $PM_{2.5}$ under polluted levels at a regional station in Northern China. Int. J. Environ. Res. Public Health 13, 1202–1207.
Liu, J., Bi, X., Li, F., Wang, P., Wu, J., 2018. Source discrimination of atmospheric metal deposition by multi-metal isotopes in the Three Gorges Reservoir region, China. Environ. Pollut. 240, 582–589.
Liu, J.Y., Liu, Z.R., Wen, T.X., Guo, J.L., Huang, X.J., Qiao, B.W., et al., 2016. Characteristics of the size distribution of water soluble inorganic ions during a typical haze pollution in the autumn in Shijiazhuang. Environ. Sci. 37, 3258–3267.
Makar, P.A., Moran, M.D., Zheng, Q., Cousineau, S., Sassi, M., Duhamel, A., et al., 2009. Modelling the impacts of ammonia emissions reductions on North American air quality. Atmos. Chem. Phys. 9, 7183–7212.
Mesquita, S.R., Dachs, J., van Drooge, B.L., Castro-Jimenez, J., Navarro-Martin, L., Barata, C., et al., 2016. Toxicity assessment of atmospheric particulate matter in the Mediterranean and Black Seas open waters. Sci. Total Environ. 545-546, 163–170.
Nakahara, A., Takagi, K., Sorimachi, A., Katata, G., Matsuda, K., 2019. Enhancement of dry deposition of $PM_{2.5}$ nitrate in a cool-temperate forest. Atmos. Environ. 212, 136–141.
Oliva, S.R., Espinosa, A.J.F., 2007. Monitoring of heavy metals in topsoils, atmospheric particles and plant leaves to identify possible contamination sources. Microchem. J. 86, 131–139.
Osada, K., Saito, S., Tsurumaru, H., Hoshi, J., 2019. Vehicular exhaust contributions to high NH_3 and $PM_{2.5}$ concentrations during winter in Tokyo, Japan. Atmos. Environ. 206, 218–224.
Pietrogrande, M.C., Dalpiaz, C., Dell'Anna, R., Lazzeri, P., Manarini, F., Visentin, M., et al., 2018. Chemical composition and oxidative potential of atmospheric coarse particles at an industrial and urban background site in the alpine region of northern Italy. Atmos. Environ. 191, 340–350.
Quan, J., Liu, Q., Li, X., Gao, Y., Jia, X., Sheng, J., et al., 2015. Effect of heterogeneous aqueous reactions on the secondary formation of inorganic aerosols during haze events. Atmos. Environ. 122, 306–312.
Roig Rodelas, R., Perdrix, E., Herbin, B., Riffault, V., 2019. Characterization and variability of inorganic aerosols and their gaseous precursors at a suburban site in northern France over one year (2015–2016). Atmos. Environ. 200, 142–157.
Saxena, M., Sharma, A., Sen, A., Saxena, P., Saraswati, Mandal T.K., et al., 2017. Water soluble inorganic species of PM_{10} and $PM_{2.5}$ at an urban site of Delhi, India: Seasonal variability and sources. Atmos. Res. 184, 112–125.
Schiferl, L.D., Heald, C.L., Van Damme, M., Clarisse, L., Clerbaux, C., Coheur, P.F., et al., 2016. Interannual variability of ammonia concentrations over the United States: sources and implications. Atmos. Chem. Phys. 16, 12305–12328.
Shang, X., Zhang, K., Meng, F., Wang, S., Lee, M., Suh, I., et al., 2018. Characteristics and source apportionment of fine haze aerosol in Beijing during the winter of 2013. Atmos. Chem. Phys. 18, 2573–2584.
Siepka, D., Uzu, G., Stefaniak, E.A., Sobanska, S., 2018. Combining Raman microspectrometry and chemometrics for determining quantitative molecular composition and mixing state of atmospheric aerosol particles. Microchem. J. 137, 119–130.
Skrbic, B., Durisic-Mladenovic, N., 2007. Principal component analysis for soil contamination with organochlorine compounds. Chemosphere 68, 2144–2152.
Sudheer, A.K., Rengarajan, R., 2015. Time-resolved inorganic chemical composition of fine aerosol and associated precursor gases over an urban environment in western India: Gas-aerosol equilibrium characteristics. Atmos. Environ. 109, 217–227.
Švédová, B., Kucbel, M., Raclavská, H., Růžičková, J., Raclavský, K., Sassmanová, V., 2019. Water-soluble ions in dust particles depending on meteorological conditions in urban environment. J. Environ. Manage. 237, 322–331.
Tan, H., Cai, M., Fan, Q., Liu, L., Li, F., Chan, P.W., et al., 2017. An analysis of aerosol liquid water content and related impact factors in Pearl River Delta. Sci. Total Environ. 579, 1822–1830.
Tang, X., Zhang, X., Ci, Z., Guo, J., Wang, J., 2016. Speciation of the major inorganic salts in atmospheric aerosols of Beijing, China: Measurements and comparison with model. Atmos. Environ. 133, 123–134.
Tang, Y., Han, G., 2017. Characteristics of major elements and heavy metals in atmospheric dust in Beijing, China. J. Geochem. Explor. 176, 114–119.
Tian, S., Pan, Y., Wang, Y., 2018. Ion balance and acidity of size-segregated particles during haze episodes in urban Beijing. Atmos. Res. 201, 159–167.
Tian, S.L., Pan, Y.P., Wang, Y.S., 2016. Size-resolved source apportionment of particulate matter in urban Beijing during haze and non-haze episodes. Atmos. Chem. Phys. 16, 1–19.
Wang, H., Ding, J., Xu, J., Wen, J., Han, J., Wang, K., et al., 2019a. Aerosols in an arid environment: The role of aerosol water content, particulate acidity, precursors, and relative humidity on secondary aerosols. Sci. Total Environ. 646, 564–572.
Wang, X., Wei, W., Cheng, S., Yao, S., Zhang, H., Zhang, C., 2019b. Characteristics of $PM_{2.5}$ and SNA components and meteorological factors impact on air pollution through 2013–2017 in Beijing, China. Atmos. Pollut. Res. 10, 1976–1984.
Wang, Z., Wu, Z., Yue, D., Shang, D., Guo, S., Sun, J., et al., 2017. New particle formation in China: Current knowledge and further directions. Sci. Total Environ. 577, 258–266.
Watson, J.G., Chow, J.C., Lurmann, F.W., Musarra, S.P., 1994. Ammonium nitrate, nitric acid, and ammonia equilibrium in wintertime Phoenix, Arizona. J. Air Waste Manage. Assoc. 44, 405–412.
Xu, L., Duan, F., He, K., Ma, Y., Zhu, L., Zheng, Y., et al., 2017. Characteristics of the secondary water-soluble ions in a typical autumn haze in Beijing. Environ. Pollut. 227, 296–305.
Xue, J., Griffith, S.M., Yu, X., Lau, A.K.H., Yu, J.Z., 2014. Effect of nitrate and sulfate relative abundance in $PM_{2.5}$ on liquid water content explored through half-hourly observations of inorganic soluble aerosols at a polluted receptor site. Atmos. Environ. 99, 24–31.
Xue, J., Lee, C., Wakeham, S.G., Armstrong, R.A., 2011. Using principal components analysis (PCA) with cluster analysis to study the organic geochemistry of sinking particles in the ocean. Org. Geochem. 42, 356–367.
Yin, S., Huang, Z., Zheng, J., Huang, X., Chen, D., Tan, H., 2018. Characteristics of inorganic aerosol formation over ammonia-poor and ammonia-rich areas in the Pearl River Delta region, China. Atmos. Environ. 177, 120–131.
Zhang, X., Zhang, K., Lv, W., Liu, B., Aikawa, M., Wang, J., 2019. Characteristics and risk assessments of heavy metals in fine and coarse particles in an industrial area of central China. Ecotox. Environ. Safe. 179, 1–8.
Zhong, C., Yang, Z., Jiang, W., Hu, B., Hou, Q., Yu, T., et al., 2016. Ecological geochemical assessment and source identification of trace elements in atmospheric deposition of an emerging industrial area: Beibu Gulf economic zone. Sci. Total Environ. 573, 1519–1526.
Zhou, M., Qiao, L., Zhu, S., Li, L., Lou, S., Wang, H., et al., 2016. Chemical characteristics of fine particles and their impact on visibility impairment in Shanghai based on a 1-year period observation. J. Environ. Sci. 48, 151–160.
Zong, Z., Wang, X., Tian, C., Chen, Y., Fu, S., Qu, L., et al., 2018. PMF and PSCF based source apportionment of $PM_{2.5}$ at a regional background site in North China. Atmos. Res. 203, 207–215.